Role of the Occluding Loop in Cathepsin B Activity*

(Received for publication, September 19, 1996, and in revised form, October 17, 1996)

Chantal Illy‡§, Omar Quraishi‡§¶, Jing Wang‡, Enrico Purisima‡, Thierry Vernet§‖, and John S. Mort§**‡‡

*From the ‡Biotechnology Research Institute, National Research Council of Canada, Montreal, Quebec H4P 2R2, Canada, the ¶Department of Biochemistry, McGill University, Montreal, Quebec H3G 1Y6, Canada, the ‖Institut de Biologie Structurale, 41 avenue des Martyrs, 38027 Cedex 1, France, the **Joint Diseases Laboratory, Shriners Hospital for Children, and Department of Surgery, McGill University, Montreal, Quebec H3G 1A6, Canada*

Within the lysosomal cysteine protease family, cathepsin B is unique due to its ability to act both as an endopeptidase and a peptidyldipeptidase. This latter capacity to remove C-terminal dipeptides has been attributed to the presence of a 20-residue insertion, termed the occluding loop, that blocks the primed terminus of the active site cleft. Variants of human procathepsin B, where all or part of this element was deleted, were expressed in the yeast *Pichia pastoris*. A mutant, where the 12 central residues of the occluding loop were deleted, autoprocessed, albeit more slowly than the wild type proenzyme, to yield a mature form of the enzyme with endopeptidase activity comparable with the wild-type cathepsin B, but totally lacking exopeptidase activity. This deletion mutant showed a 40-fold higher affinity for the inhibitor cystatin C, suggesting that the occluding loop normally restricts access of this inhibitor to the active site. In addition, the binding affinity of the cathepsin B propeptide, which is a potent inhibitor of this enzyme, was 50-fold increased, consistent with the finding that the loop reorients on activation of the proenzyme. These results suggest that the endopeptidase activity of cathepsin B is an evolutionary remnant since, as a consequence of its membership in the papain family, the propeptide must be able to bind unobstructed through the full length of the active site cleft.

The lysosomal cysteine protease cathepsin B is unique within the papain superfamily in that it acts both as an endopeptidase and an exopeptidase. Thus in addition to making internal cleavages (1), it also removes C-terminal dipeptide units from the substrate (peptidyldipeptidase activity) (2). The x-ray crystal structure of cathepsin B suggests the molecular basis for this dual character. Relative to other papain-like proteases, cathepsin B contains an extra structural element termed the "occluding loop" (3), which blocks off one end of the substrate binding cleft (see Fig. 1*a*). As proposed by Schechter and Berger (4), the protease active site cleft is considered to consist of a series of subsites, each accommodating an amino acid residue of the peptide substrate. Those subsites binding the residues C-terminal to the peptide bond undergoing cleavage are termed the primed sites (S_1' to S_3') and accept the P_1' to P_3' substrate residues. The subsites accepting the N-terminal side of the substrate, the P_1 to P_3 residues, are termed the unprimed sites (S_1 to S_3, with the numbering in each case starting with the residues bordering the cleavage site). The structure of rat cathepsin B containing the covalently bound inhibitor Z-Arg-Ser(OBz)-chloromethylketone (where Z represents benzyloxycarbonyl and Bz represents benzoyl) (5) maps out the unprimed substrate binding subsites and indicates that the occluding loop plays a defining role in primed site specificity. The strategic position of two histidine residues in this loop (His[110] and His[111])[1] suggests that they can act as acceptors for the negatively charged carboxylate of the P_2' residue C terminus. The structure of a human cathepsin B complex with the E-64[2] analogue CA030 (the ethyl ester of epoxysuccinyl-Ile-Pro-OH) (6) shows this can indeed be the case. The free carboxyl group on the proline residue in the dipeptide moiety of this inhibitor interacts with these two histidines suggesting that Ile and Pro occupy the P_1' and P_2' subsites, respectively, as would be expected for substrate binding in the exopeptidase mode.

While the occluding loop appears to play an important role in the binding of substrates that are cleaved by the exopeptidase activity of cathepsin B, it would be expected to interfere with the binding of extended peptides. It would also be expected to obstruct the binding of protein protease inhibitors such as the cystatins, which in the case of the papain/stefin B complex have been shown to form extensive interactions with the protease primed sites (7). Since the occluding loop represents a separate and relatively poorly ordered region of cathepsin B (5), we reasoned that it could be deleted without compromising the structure of the remaining enzyme.

We have previously demonstrated the efficient recombinant expression of rat cathepsin B as an α-factor fusion construct in the yeast *Saccharomyces cerevisiae* (8). This system proved much less effective for the expression of the human enzyme (9); however, we have recently shown that high levels of human cathepsin B can be produced using similar constructs in the methanotropic yeast *Pichia pastoris* (10). We have used this system to produce forms of human cathepsin B lacking the occluding loop and thus allowing us to evaluate its role in cathepsin B function.

[1] Residue numbering relates to mature cathepsin B.
[2] The abbreviations used are: E-64, *trans*-epoxysuccinyl-L-leucyl-amido-(4-guanidino)butane; Z-Phe-Arg-MCA, benzyloxycarbonyl-L-phenylalanyl-L-arginine 4-methylcoumarinyl-7-amide; PAGE, polyacrylamide gel electrophoresis; DMSO, dimethyl sulfoxide; DTT, dithiothreitol.

EXPERIMENTAL PROCEDURES

Computer Modelling—The x-ray structures of cathepsin B (Protein Data Bank code 1cst (5)) and papain (Protein Data Band code 9pap (11)) formed the basis for structural modelling. The Kollman all atom force field and Powell minimizer were used with the program SYBYL 6.1 (Tripos Assoc. Inc.). The non-bonded cutoff was set at 8 Å and the dielectric constant to 80. The segment Cys^{108} to Cys^{119} in the cathepsin B occluding loop was deleted, and the remaining ends were joined through a peptide linkage (mutant M1, see Fig. 1, *a* and *c*). Energy minimizations were performed allowing Ser^{104} to Asp^{124} and residues within 8 Å to move, while the rest of the molecule remained fixed. The minimizations were judged to be complete when the root mean square of the gradients was smaller than 0.1 kcal/mol Å.

Construction of Human Cathepsin B Deletion Mutants—A cDNA construct, consisting of wild-type human procathepsin B as a fusion with the preproregion of yeast α-factor, had been prepared previously in pVT105 (a derivative of the multiple purpose yeast shuttle vector pVT100U (12), where the ADH promoter had been deleted). The consensus sequence for oligosaccharide substitution in the mature protein had been removed by the substitution S115A (9). *Xho*I and *Not*I restriction sites were then introduced into the C-terminal region of the α-factor proregion and the 3′-untranslated region of procathepsin B, respectively, to allow subcloning into the *P. pastoris* expression vector pPIC9 (Invitrogen). Using single-stranded DNA from the construct in pVT105, two deletion mutants of human procathepsin B were constructed by loop-out mutagenesis. The oligonucleotide 5′-CCG TAC TCC ATC CCT CCC ACG GGG GAG GGA GAT ACC-3′ was used to remove Cys^{108} to Cys^{119}, yielding the mutant M1 (see Fig. 1*c*). The oligonucleotide 5′-GTA GGG TGC AGA CCG TAC GAA GGT GTT CAA AAG TGT AGC AAA ATC TGT G-3′ was used to delete residues Ser^{104} to Pro^{126} and add four amino acids from the papain sequence (Glu^{89}-Gly^{90}-Val^{91}-Gln^{92}) as a linker, giving the mutant M2 (Fig. 1*d*). Sequencing of the complete procathepsin B cDNA inserts following mutagenesis confirmed the expected sequences. Both constructs were digested with *Xho*I and *Not*I, and the procathepsin B fragment was subcloned into pPIC9.

Expression of Mutants in P. pastoris—For integration into the *Pichia* genome, the pPIC9 based constructs were linearized by cleavage with *Bgl*II and purified. The *P. pastoris* host strain GS115 (Invitrogen) was then transformed with the linearized constructs by electroporation. Positive transformants were grown for 2 days in medium containing glycerol as the carbon source followed by growth in the presence of methanol for a further 2 days to induce expression of recombinant protein. Protein secreted into the culture supernatants was analyzed by SDS-PAGE and Western blotting using sheep anti-human cathepsin B (13).

Purification of M1 and M2 Mutant Proteins—After concentration, supernatants were dialyzed against 50 mM sodium acetate, 1 mM EDTA (pH 5.0) to allow autoprocessing of proenzyme mutants. The mature mutant M1 was reversibly inactivated by addition of methylmethane-thiosulfonate (1 mM) and purified on an FPLC system (Pharmacia) using an SP-Sepharose fast flow column. The enzyme eluted with 150 mM NaCl. Mutant M2, which was not able to autoprocess, was purified in its proenzyme form using an SP-Sepharose fast flow column under the conditions described above. The proenzyme form of mutant M1 was purified by gel filtration chromatography using a Sephacryl 200HR column equilibrated in 25 mM Tris, 150 mM NaCl (pH 7.5).

Active Site Titration—The concentration of active wild-type enzyme was determined by titration using the cysteine protease inhibitor E-64 (Sigma) (14). The mutant M1 proved to be poorly inhibited by E-64, so enzyme concentrations were estimated by titration with recombinant human cystatin C prepared as described previously (15).

Enzyme Assays—Endopeptidase activity was determined spectrofluorometrically using the fluorogenic amidomethylcoumaryl substrate Z-Phe-Arg-MCA. Methylcoumarinyl-7-amide release was monitored at 25 °C on a SPEX Fluorolog-2 spectrofluorometer at 440 nm using an excitation wavelength of 380 nm. Two different buffers were used: 50 mM sodium acetate (pH 5.2), containing 200 mM NaCl, 1 mM EDTA, 2 mM DTT, and 1% acetonitrile, and 50 mM sodium phosphate (pH 6.0), containing 1 mM EDTA, 200 mM NaCl, 2 mM DTT, and 3% DMSO. The values of k_{cat} and K_m were determined using non-linear regression analysis (16).

The exopeptidase activity was measured using the synthetic substrate dansyl-Phe-Arg-Phe(NO$_2$)-Leu, which was prepared as described by Pohl *et al.* (17) except that Fmoc (*N*-(9-fluorenyl)methoxycarbonyl) chemistry was used. Assay conditions were 10 μM substrate, in 25 mM sodium citrate (pH 5.0) containing 0.25 M NaCl, 1 mM EDTA, 3% DMSO,

2 mM DTT at 25 °C. Dansyl release was monitored by excitation at 350 nm and emission at 535 nm.

The proteolytic activity of cathepsin B mutants against protein substrates was performed using azocasein (18) in 50 mM sodium acetate (pH 5.2), containing 200 mM NaCl, 1 mM EDTA, 2 mM DTT. After incubation at 30 °C for 30 min with 0.5% azocasein, proteins were trichloroacetic acid-precipitated, and A_{366} of the supernatants containing liberated peptides was measured.

pH Activity Profiles—k_{cat}/K_m values were measured at 0.1 pH intervals over the range of pH 3.0–8.4 based on the relationship $v = [E][S] k_{cat}/K_m$ at $[S] \ll K_m$. The reaction buffers were 50 mM sodium citrate (pH 3.0–6.0), 50 mM sodium phosphate (pH 5.8–7.8), and 25 mM sodium borate (pH 7.7–8.4). All buffers contained 200 mM NaCl, 1 mM EDTA, and 2 mM DTT. The pH for each reaction was checked immediately after measurement of the initial rate.

Thermostability Measurements—Cathepsin B (0.7 nM) in 50 mM sodium acetate buffer (pH 5.2) containing 200 mM NaCl, 1 mM EDTA was incubated at 20 or 30 °C for various times. The remaining enzymatic activity was measured using the same buffer system containing 2 mM DTT, 1% acetonitrile, and 5 μM Z-Phe-Arg-MCA.

Interaction of Cystatin C with M1 Mutant and Wild-type Cathepsin B—Enzymes and human cystatin C were incubated either in 50 mM sodium acetate buffer (pH 5.2), containing 200 mM NaCl, 1 mM EDTA, 2 mM DTT, and 1% acetonitrile, or in 50 mM sodium phosphate (pH 6.0), containing 1 mM EDTA, 200 mM NaCl, 2 mM DTT, and 3% DMSO, for 5 min at room temperature. The residual enzyme activity was measured using 5 μM Z-Phe-Arg-MCA. Values of K_i were calculated by non-linear regression analysis using the general equation describing tight binding inhibition. Precise cystatin C concentrations were determined by titration with papain (19).

Inhibition by the Cathepsin B Propeptide—The rat cathepsin B propeptide (PCB1, residues 1-56) was prepared as described previously (20). Inhibition experiments were performed either in 50 mM sodium acetate (pH 5.2), 200 mM NaCl, 1 mM EDTA, 2 mM DTT, 1% acetonitrile or in 50 mM sodium phosphate (pH 6.0), 100 mM NaCl, 0.2 mM EDTA, 2 mM DTT, 0.025% DMSO using 5 μM Z-Phe-Arg-MCA as substrate. Under these conditions, progress curves for the inhibition of the mutant M1 and wild-type cathepsin B by PCB1 at pH 5.2 and 6.0 followed typical slow-binding kinetics as defined by the equation,

$$[P] = v_s t + [(v_i - v_s)(1 - \exp(-k_{obs}t))]/k_{obs}$$

where *P* is the product formed, v_i and v_s are the initial and steady-state velocities, respectively, *t* is the reaction time, and k_{obs} is the apparent second order rate constant for inhibition. Nonlinear regression analysis using the program Enzfitter (Elsevier-Biosoft, Cambridge, U. K.) gave the individual parameters (v_i, v_s and k_{obs}) for each progress curve. For each data set, the enzyme-inhibitor dissociation constant (K_i) values were obtained from the relationship $v_i/v_s - 1 = [I]/K_i$ (21). The plot of k_{obs} *versus* [I] remained linear over the range of inhibitor concentrations studied (2–20 nM), giving an estimate of k_{on} and confirming that inhibition by PCB1 occurred by a one-step process (20). The dissociation rate constant k_{off} was calculated from the relationship $K_i = k_{off}/k_{on}$.

SDS-PAGE Analysis—Proteins were treated with 10 μM of E-64. When necessary, they were deglycosylated with endoglycosidase H. After precipitation with methanol (4 volumes), deglycosylation was performed in 25 mM sodium citrate buffer (pH 5.0) by incubation with 1 unit of endoglycosidase H (Boehringer Mannheim) for 1 h at 37 °C. Proteins were analyzed by gel electrophoresis (12%) in the presence of SDS under reducing conditions.

RESULTS

Modelling of Cathepsin B Occluding Loop Mutants—The possibility that the cathepsin B occluding loop could be deleted without causing significant perturbation of the remaining protein was investigated by molecular modelling. Inspection of the x-ray crystal structure of cathepsin B suggested that the disulfide-bonded segment, Cys^{108} to Cys^{119}, could be deleted and a peptide bond formed between Pro^{107} and Thr^{120} (Fig. 1*c*). Energy minimization of the resulting structure, the mutant M1 (Fig. 1*a*), showed that, on the formation of this bond, only a few residues on the surface of the molecule would be displaced, suggesting that deletion of this segment would not seriously affect the overall structure of the molecule.

Relative to papain, which lacks the occluding loop, the mutant M1 still included eight residues of this structural element.
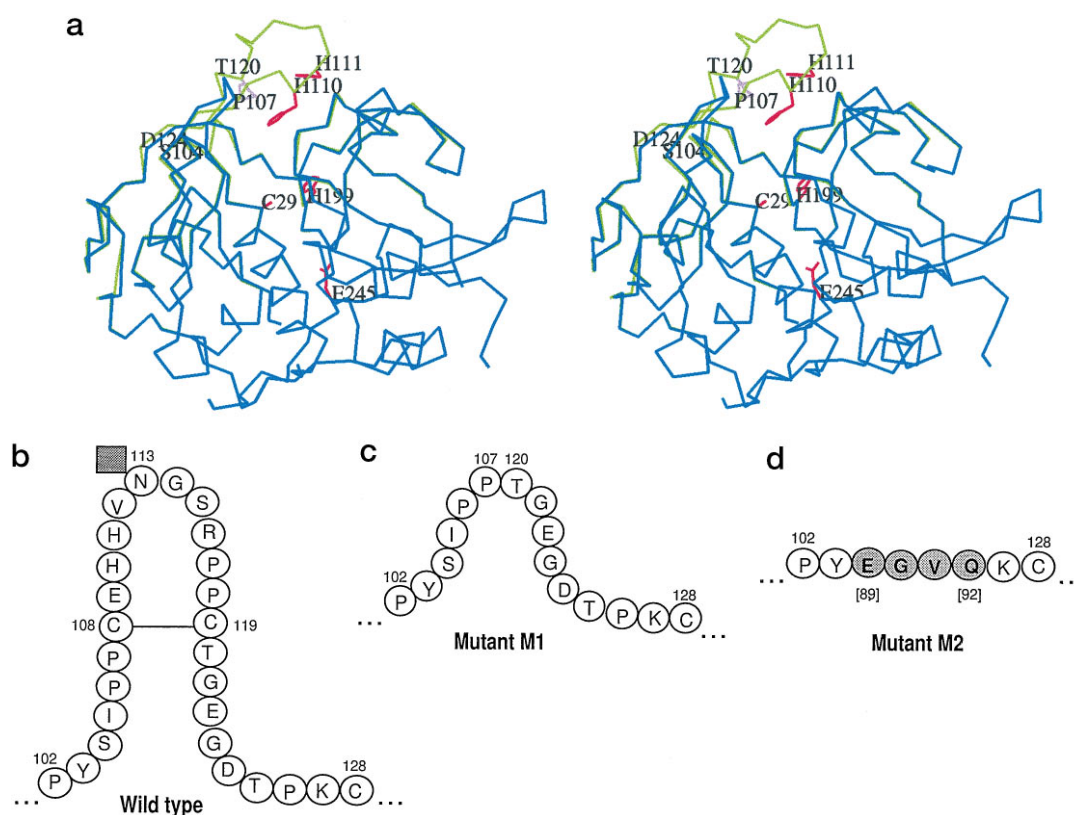
FIG. 1. **Occluding loop mutants of cathepsin B**. *a,* stereo view of the α-carbon trace of wild-type human cathepsin B (*green*) superimposed on a modelled structure of the mutant M1 (*blue*). Areas of complete overlap are also shown in *blue*. The disulfide bond between Cys[108] and Cys[119] is shown in *pink*. The side chains of residues involved in substrate binding and catalysis (Glu[245], His[110], His[111], Cys[29], and His[199]) are shown in full. The positions of residues delimiting the occluding loop mutants M1 (Pro[107] and Thr[120]) and M2 (Ser[104] and Asp[124]) are also indicated. *b,* schematic representation of the occluding loop of wild-type cathepsin B. The *filled square* on Asn[113] represents the site of *N*-linked oligosaccharide substitution that was deleted in the wild-type enzyme used in this study due to the substitution S115A. *c,* schematic representation of mutant M1 indicating the junction between Pro[107] and Thr[120]. *d,* schematic representation of mutant M2 showing the points of deletion and position of the tetrapeptide Glu-Gly-Val-Gln (*gray background*), corresponding to residues 89–92 of papain, inserted in the place of residues 123–126.

For the complete deletion, the segment 104–126 was removed, and the resulting gap closed using a connecting tetrapeptide derived from the homologous region of papain (Fig. 1*d*). Superimposition of the modified cathepsin B structure (the mutant M2) with that of papain suggested that these changes could be accommodated without radical restructuring of the protein. Energy minimization of this more drastically modified form was not attempted.

Expression and Purification of the Procathepsin B Mutants— Deletion of part or all of the occluding loop was accomplished by loop-out mutagenesis. Both mutant proteins were expressed and secreted at levels comparable with the wild-type human enzyme (approximately 20 mg/liter of culture medium) and as previously observed for rat procathepsin B (10). The mutant M1 precursor was purified by gel filtration, and the proenzyme form of the mutant M2 was purified by ion exchange chromatography. About 10 mg of pure proenzymes were obtained in each case (Fig. 2). The recombinant cathepsin B proenzymes expressed in *P. pastoris* were heterogeneous due to modification of the *N*-linked oligosaccharide moiety on the proregion and migrated with apparent molecular masses ranging from 40 to 52 kDa with a dominant band at the leading edge of the smear (Fig. 2, *lanes 1* and *5*). Following enzymatic deglycosylation with endoglycosidase H, each cathepsin B form resolved as a single band of the expected size of 36.5 kDa (Fig. 2, *lanes 2* and *6*), migrating slightly faster than the deglycosylated wild-type proenzyme. The far UV circular dichroism spectra of the mutant proenzymes were similar to that of the wild-type proenzyme, suggesting correct folding (data not shown).

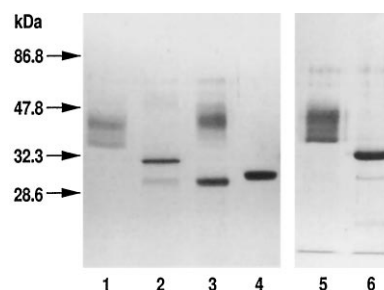*In Vitro Processing of the M1 and M2 Mutants—*Wild-type

FIG. 2. **SDS-PAGE of purified mutants M1 and M2 (Coomassie Blue staining).** *Lane 1,* proenzyme M1; *lane 2,* deglycosylated proenzyme M1; *lane 3,* mature M1 after processing (still containing a small amount of proenzyme); *lane 4,* mature wild-type human cathepsin B; *lane 5,* proenzyme M2; and *lane 6,* deglycosylated proenzyme M2. Positions of molecular mass standards are indicated on the *left*.

procathepsin B is readily processed upon activation at acid pH (9), leading to the generation of the mature, active, single chain form of the enzyme (Fig. 2, *lane 4*). Processing of the M1 precursor to yield a proteolytically active enzyme proceeded at a much slower rate than that observed for the wild-type enzyme (Fig. 2, *lane 3*). Five days at pH 5.0 were required to totally activate the mutant M1, whereas the wild type enzyme was completely processed following overnight dialysis at 4 °C. Processing was accelerated somewhat under lower pH conditions. Inclusion of the cysteine protease inhibitor, E-64, during dialysis prevented maturation of the precursor, suggesting that activation occurred as the result of autoprocessing. N-terminal sequencing demonstrated a three residue extension relative to
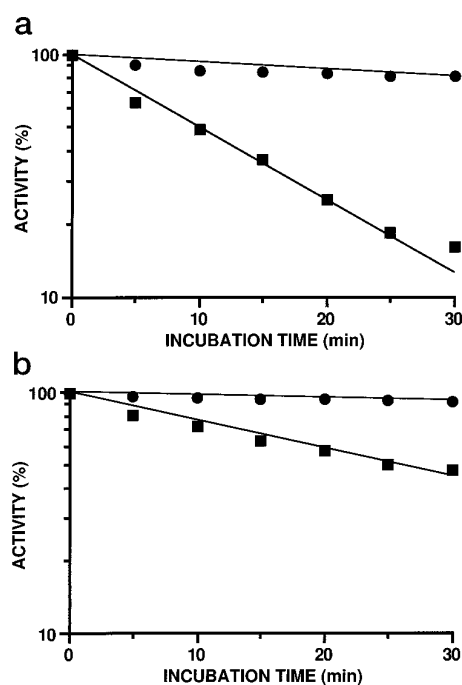
FIG. 3. **Thermal inactivation of mutant M1 and wild-type cathepsin B.** Enzymes were preincubated at pH 5.2 for the times indicated at 30 °C (*a*) or at 20 °C (*b*) and then assayed for endopeptidase activity using Z-Phe-Arg-MCA. Mutant M1 (■); wild-type cathepsin B (●).

TABLE I

Kinetic constants for the hydrolysis of Z-Phe-Arg-MCA by mutant M1 and wild-type cathepsin B

Enzyme	k_{cat} (s^{-1})	K_m (mM)	k_{cat}/K_m (M^{-1} s^{-1})
pH 5.2			
Wild-type	41.3 ± 6.1	0.110 ± 0.010	$375,000 \pm 31,000$
Mutant M1	6.89 ± 1.4	0.0212 ± 0.002	$327,000 \pm 26,000$
pH 6.0			
Wild-type	42.2 ± 7.0	0.105 ± 0.009	$422,000 \pm 29,000$
Mutant M1	4.44 ± 1.1	0.0179 ± 0.003	$261,000 \pm 22,000$

TABLE II

Activity of mutant M1 and wild-type cathepsin B towards azocasein

Enzymes were incubated with azocasein in the buffer 50 mM sodium acetate (pH 5.2), 200 mM NaCl, 1 mM EDTA for 1 h at 20 °C or 30 minutes at 30 °C. For reaction in the presence of E-64, enzymes were preincubated with the inhibitor (10 μM) for 5 min before assay.

Enzyme	Specific activity
	μg of azocasein degraded/mg of enzyme/min
20 °C	
Wild-type	262 ± 15
Mutant M1	150 ± 16
30 °C	
Wild-type	480 ± 8
Mutant M1	422 ± 9
Wild-type + E-64	15 ± 0.2
Mutant M1 + E-64	18 ± 0.2

the fully processed lysosomal form. Attempts to process the mutant M1 using extrinsically added proteases (pepsin, papain, and proteinase K) were unsuccessful as the protein was either totally resistant or rapidly degraded (data not shown).

The mature mutant M1 was purified by ion-exchange chromatography on an SP-Sepharose column. From 1 liter of culture medium, 4 mg of pure mature M1 could be obtained, which migrated as a single band with a slightly higher mobility than wild-type cathepsin B (Fig. 2, *lane 3*). The mutant M2 did not autoprocess at acidic pH, even following lengthy incubation at 37 °C. Processing could be attained in the presence of exogenous wild-type cathepsin B but not with other extrinsically added proteases such as pepsin, papain, or proteinase K. This conversion was shown to be both time- and dose-dependent as in the case of rat procathepsin B (C29S) (8). Further characterization of the mature mutant M2 was not carried out due to the inability to separate it from the wild-type cathepsin B used for processing.

Thermal Inactivation of the Mature M1 Mutant—The mutant M1 was found to be much more sensitive to thermal inactivation than the wild-type enzyme (Fig. 3). Loss of activity followed simple first order kinetics. At 30 °C, inactivation of the mutant M1 occurred with a $t_{1/2}$ of 11 min compared with 110 min for the wild-type enzyme. A similar differential effect was seen at 20 °C ($t_{1/2}$ of 28 and 280 min, respectively).

Endo- and Exopeptidase Activities of the M1 Mutant—Kinetic analysis was carried out with synthetic and protein substrates. Kinetic parameters, determined using the amidomethylcoumaryl substrate, Z-Phe-Arg-AMC, showed that removal of the external part of the loop had no significant effect on the k_{cat}/K_m value at pH 5.2 (Table I) although both K_m and k_{cat} showed a 5-fold decrease for the mutant M1 compared with the wild-type enzyme. At pH 6.0, k_{cat}/K_m was about 1.6-fold lower for the mutant M1 (Table I), consistent with a decrease in k_{cat} at this pH. Little change in K_m was observed between pH 5.2 and 6.0.

Activity of the mutant M1 was also tested against the protein

substrate, azocasein (Table II). The deletion mutant was able to cleave this substrate with a specific activity similar to that of the wild-type enzyme. This activity was completely abolished in the presence of the cysteine protease inhibitor E-64. These estimates of the proteolytic activity of the mutant M1 are probably underestimates since, as shown in Fig. 3, there were substantial activity losses during the incubation times used in these assays.

The peptidyldipeptidase activity of the mutant M1 was measured using the quenched fluorescence substrate dansyl-Phe-Arg-Phe(NO$_2$)-Leu. Under the experimental conditions used, no exopeptidase activity was detectable for the mutant M1 in acetate or citrate buffers at pH 5.0, while native cathepsin B showed activity (k_{cat}/K_m of 432,000 M^{-1} s^{-1}) comparable with that determined previously by Pohl *et al.* (17).

pH Activity Profiles Using the Substrate Z-Phe-Arg-MCA—As shown previously, wild-type cathepsin B exhibits a complex pH-activity profile that can best be fitted to a model involving five dissociation events, three in the ascending limb and two in the descending limb (22). Deletion of the occluding loop had a dramatic effect on the pH-activity profile (Fig. 4). Maximal activity was observed at pH 5, while the high levels of activity found for wild-type cathepsin B at pH 7–8 were not found with the mutant M1. Below pH 4.5, the activity dropped very rapidly. This loss of activity was in part the result of the reduced stability of the mutant M1 at acidic pH.

Inhibition of the M1 Mutant by Human Cystatin C—Since it had been proposed that the occluding loop of cathepsin B would obstruct the binding of cystatins to the active site (7), inhibition of the mutant M1 by human cystatin C was studied. At pH 6.0, a K_i value of 0.17 nM for the wild-type cathepsin B/cystatin C interaction was found, consistent with values obtained by others (23, 24) (Table III). However, the mutant M1 exhibited a 40-fold higher affinity for the inhibitor. The same differential effect was observed at pH 5.2. However, the affinity of both forms of the enzyme for the inhibitor was lower than at the higher pH.

Inhibition of M1 Mutant by the Synthetic Propeptide of Cathepsin B—The propeptide of cathepsin B is a potent inhibitor of the mature enzyme (20). The recently determined procathep-
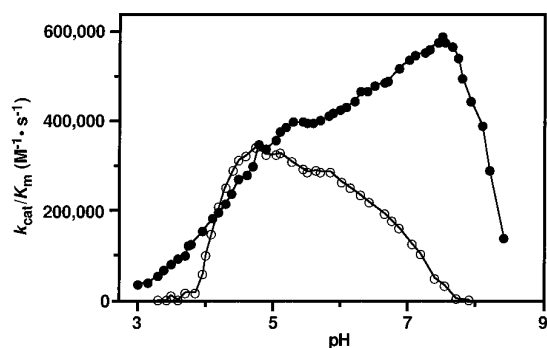
FIG. 4. **pH activity profiles of mutant M1 and wild-type human cathepsin B.** Activity was measured using Z-Phe-Arg-MCA. Wild-type cathepsin B (●); mutant M1 (○).

TABLE III

Dissociation constants for the inhibition of mutant M1 or wild-type human cathepsin B by wild-type human cystatin C

Enzyme	K_i (nM) (pH 5.2)	K_i (nM) (pH 6.0)
Wild-type	5.2 ± 0.7	0.17 ± 0.05
Mutant M1	0.18 ± 0.02	0.004 ± 0.0008

TABLE IV

Equilibrium and kinetic data for the interactions between human wild-type cathepsin B or mutant M1 and the cathepsin B propeptide

Enzyme	K_i (nM)	k_{on} (M^{-1} s^{-1})	k_{off} (s^{-1})
pH 5.2			
Wild-type	7.0 ± 0.4	0.3×10^5	2.1×10^{-4}
Mutant M1	0.2 ± 0.023	7.2×10^5	1.4×10^{-4}
pH 6.0			
Wild-type	5.4 ± 0.6	0.5×10^5	2.7×10^{-4}
Mutant M1	0.1 ± 0.03	20.2×10^5	2.0×10^{-4}

sin B structure (25, 26) indicates the occluding loop adopts a different conformation in the proenzyme so that the propeptide is able to bind through the entire active site cleft. Such a reorientation of the occluding loop must occur for the free propeptide to bind to the mature enzyme. In agreement with this proposal, the affinity of the free cathepsin B propeptide for the mutant M1 was found to be 54-fold higher than for the wild-type enzyme at pH 6.0 (Table IV). A similar differential effect was seen at pH 5.2. In agreement with the proposal that the occluding loop must be reoriented during propeptide binding, the on rate is increased in the case of the mutant M1, whereas the off rate is essentially unchanged.

DISCUSSION

The occluding loop of cathepsin B represents a unique structural element relative to the other members of the papain superfamily. The three-dimensional structures of cathepsin B (3) and of a cathepsin B complex with an inhibitor occupying the S$_1'$ and S$_2'$ subsites (6) provide clues with respect to the exopeptidase activity. However, the relationship of the loop to endopeptidase activity is not clear. In order to study the role of the occluding loop, we have expressed a mutant of cathepsin B (M2) engineered to mimic the local structure of the other members of the papain superfamily. Although the folding of the precursor of this cathepsin B mutant did not appear to be altered significantly, as shown by circular dichroism spectroscopy (data not shown), this mutant did not autoprocess. In contrast, a more subtle deletion (M1) did allow processing to occur, albeit at a reduced rate relative to the wild-type precursor. Since the activation of wild type and mutant M1 procathepsin B proceeds by an autoactivation mechanism, the inability of the mutant M2 to undergo processing may be related to a stronger binding of the propeptide to the active site region. The slower autoprocessing of the mutant M1 and its higher affinity for the free propeptide support this proposal.

Studies of the mature mutant M1 provide insight into the functional role of the loop. Its partial truncation reduced the stability of the molecule indicating that this structural element contributes to the stability of the protein. In fact, the three dimensional structure of cathepsin B shows that, while the loop is attached to the left domain of the enzyme, residues 108–119 interact with the right domain, suggesting that this region of the protein may be stabilized by interdomain interactions. In

this regard, it was shown previously that interdomain perturbation in papain affects enzyme stability (27).

The three-dimensional structure also suggested an explanation of the unique ability of cathepsin B to act as an exopeptidase (3, 6). Indeed, while the mutant M1 was proteolytically active, it showed no detectable exopeptidase activity, validating the previously proposed role of the loop residues His[110] and His[111] as "acceptors" for the negative charge on the substrate P terminus. On the other hand, the K_m for the endopeptidase substrate Z-Phe-Arg-MCA decreased five-fold, showing that the peptide is able to bind to the active site in a more efficient manner. Similar endoprotease activity against a protein substrate for the wild type and M1 was demonstrated although the value for the mutant M1 is likely to have been an underestimate due to its reduced stability.

High molecular weight inhibitors also provide a method to probe active site accessibility. The recently determined three-dimensional structures of rat (25) and human (26) procathepsin B reveal that the occluding loop is a mobile element. In the precursor molecule, the loop adopts an alternate conformation to that occupied in the mature enzyme, no longer impeding access to the primed side of the active site cleft. Indeed, the free cathepsin B propeptide must trigger a similar conformational transition on binding to the mature enzyme as it is a potent, specific inhibitor of cathepsin B (20) implying that it has the ability to displace the occluding loop. This finding also implies that shortening the loop should increase the binding affinity of the free propeptide to cathepsin B, a prediction confirmed on removal of 12 residues of the loop in the mutant M1 which enhanced the affinity of the free propeptide by more than 50-fold over that for the wild-type enzyme. As expected from the mechanism of the interaction, the on rate is increased while the off rate remains essentially unchanged.

It was pointed out previously that the conformation of the occluding loop in mature cathepsin B is incompatible with cystatin binding (3), as reflected by the high K_i value for formation of the cystatin C/cathepsin B complex relative to that of cysteine proteases lacking the occluding loop (28). This is a similar situation to that described above for the binding of the propeptide and suggests that a significant alteration of the loop position occurs when the inhibitor binds to the cathepsin B active site. Indeed, partial deletion of the loop, as in the mutant M1, increases the affinity of cathepsin B for cystatin C by over 40-fold relative to the wild-type enzyme, a value similar to that found for propeptide inhibition. The K_i value for the mutant M1 approaches that reported for cathepsin L (23), a cysteine protease lacking the occluding loop. All of these kinetic and structural observations are consistent with the predictions from molecular modelling of increased access to the active site on deletion of the loop.

Although the influence of the loop on the active site accessibility is clear, the occluding loop also has an influence on the hydrolytic activity of cathepsin B. For instance, the reduction of k_{cat} by over 6-fold at pH 5.2 for the mutant M1 shows that the gain of binding efficiency (lower K_m) is offset by a reduction in substrate turnover. Also, modification of the loop lowers the

optimal pH of activity by over 2.5 pH units although the exact meaning of this effect remains obscure. The lack of symmetry of the pH-activity profile of wild-type cathepsin B has been attributed to the proximity of the loop and the protonation state of residues His[110] and His[111] (22). Shortening of the loop with the consequent removal of these two residues promotes a more symmetrical profile. Taken together, these data show the dramatic effect of the loop on the mechanism of activity.

Besides its demonstrated role in exopeptidase activity, the occluding loop of the cathepsin B clearly limits access of macromolecules to the active site. It is interesting to speculate on the evolution of cathepsin B from an ancestral papain-like cysteine protease (29). The addition of the occluding loop to facilitate peptidyldipeptidase activity had to remain compatible with the propeptide binding pattern and activation mechanism common to this family of enzymes, as demonstrated by the structures of procathepsin B and procathepsin L (25, 30). We propose, therefore, that the endoprotease activity retained by cathepsin B is an evolutionary remnant and that the main role of cathepsin B in its natural environment, the lysosome, is to act as an exopeptidase. The residual endopeptidase activity, while not essential intracellularly, still allows the enzyme to play an extracellular role as an endopeptidase that is poorly inhibited by cystatins (31). This may have important pathological consequences.

REFERENCES

1. Fosang, A. J., Neame, P. J., Last, K., Hardingham, T. E., Murphy, G., and Hamilton, J. A. (1992) *J. Biol. Chem.* **267,** 19470–19474
2. Aronson, N. N., and Barrett, A. J. (1978) *Biochem. J.* **171,** 759–765
3. Musil, D., Zucic, D., Engh, R. A., Mayr, I., Huber, R., Popovic, T., Turk, V., Towatari, T., Katunuma, N., and Bode, W. (1991) *EMBO J.* **10,** 2321–2330
4. Schechter, I., and Berger, A. (1967) *Biochem. Biophys. Res. Commun.* **27,** 157–162
5. Jia, Z., Hasnain, S., Hirama, T., Lee, X., Mort, J. S., To, R., and Huber, C. P. (1995) *J. Biol. Chem.* **270,** 5527–5533
6. Turk, D., Podobnik, M., Popovic, T., Katunuma, N., Bode, W., Huber, R., and Turk, V. (1995) *Biochemistry* **34,** 4791–4797
7. Stubbs, M. T., Laber, B., Bode, W., Huber, R., Jerala, R., Lenarcic, B., and Turk, V. (1990) *EMBO J.* **9,** 1939–1947
8. Rowan, A. D., Mason, P., Mach, L., and Mort, J. S. (1992) *J. Biol. Chem.* **267,** 15993–15999
9. Mach, L., Mort, J. S., and Glössl, J. (1994) *J. Biol. Chem.* **269,** 13030–13035
10. Sivaraman, J., Coulombe, R., Magny, M.-C., Mason, P., Mort, J. S., and Cygler, M. (1996) *Acta Crystallogr. Sec. D* **52,** 874–875
11. Kamphuis, I. G., Kalk, K. H., Swerte, M. B. A., and Drenth, J. (1984) *J. Mol. Biol.* **179,** 233–256
12. Vernet, T., Dignard, D., and Thomas, D. Y. (1987) *Gene* (*Amst.*) **52,** 225–233
13. Mort, J. S., Poole, A. R., and Decker, R. S. (1981) *J. Histochem. Cytochem.* **29,** 649–657
14. Barrett, A. J., and Kirschke, H. (1981) *Methods Enzymol.* **80,** 535–561
15. Lindahl, P., Abrahamson, M., and Björk, I. (1992) *Biochem. J.* **281,** 49–55
16. Leatherbarrow, R. J. (1990) *Trends Biochem. Sci.* **15,** 455–458
17. Pohl, J., Davinic, S., Blaha, I., Strop, P., and Kostka, V. (1987) *Anal. Biochem.* **165,** 96–101
18. Starkey, P. M. (1977) in *Proteinases in Mammalian Cells and Tissues* (Barrett, A. J., ed) pp. 57–89, Elsevier/North Holland, Amsterdam
19. Lindahl, P., Alriksson, E., Jörnvall, H., and Björk, I. (1988) *Biochemistry* **27,** 5074–5082
20. Fox, T., de Miguel, E., Mort, J. S., and Storer, A. C. (1992) *Biochemistry* **31,** 12571–12576
21. Izquierdo-Martin, M., and Stein, R. L. (1992) *J. Am. Chem. Soc.* **114,** 1527–1528
22. Hasnain, S., Hirama, T., Tam, A., and Mort, J. S. (1992) *J. Biol. Chem.* **267,** 4713–4721
23. Abrahamson, M., Mason, R. W., Hansson, H., Buttle, D. J., Grubb, A., and Ohlsson, K. (1991) *Biochem. J.* **273,** 621–626
24. Lindahl, P., Ripoll, D., Abrahamson, M., Mort, J. S., and Storer, A. C. (1994) *Biochemistry* **33,** 4384–4392
25. Cygler, M., Sivaraman, J., Grochulski, P., Coulombe, R., Storer, A. C., and Mort, J. S. (1996) *Structure* **4,** 405–416
26. Turk, D., Podobnik, M., Kuhelj, R., Dolinar, M., and Turk, V. (1996) *FEBS Lett.* **384,** 211–214
27. Vernet, T., Tessier, D. C., Khouri, H. E., and Altschuh, D. (1992) *J. Mol. Biol.* **224,** 501–509
28. Björk, I., Pol, E., Raub-Segall, E., Abrahamson, M., Rowan, A. D., and Mort, J. S. (1994) *Biochem. J.* **299,** 219–225
29. Berti, P. J., and Storer, A. C. (1995) *J. Mol. Biol.* **246,** 273–283
30. Coulombe, R., Grochulski, P., Sivaraman, J., Ménard, R., Mort, J. S., and Cygler, M. (1996) *EMBO J.* **15,** 5492–5503
31. Barrett, A. J., Buttle, D. J., and Mason, R. W. (1988) *ISI Atlas of Sci: Biochem.* 256–260

Role of the Occluding Loop in Cathepsin B Activity

Chantal Illy, Omar Quraishi, Jing Wang, Enrico Purisima, Thierry Vernet and John S. Mort

Access the most updated version of this article at http://www.jbc.org/content/272/2/1197

Alerts:
- When this article is cited
- When a correction for this article is posted

Click here to choose from all of JBC's e-mail alerts

This article cites 29 references, 9 of which can be accessed free at
http://www.jbc.org/content/272/2/1197.full.html#ref-list-1